Supporting Information

A Trustworthy CpG Nanoplatform for Highly Safe and Efficient Cancer Photothermal Combined Immunotherapy

Jiang Ming,[#a] Jinjia Zhang,[#b] Yiran Shi,[b] Wangheng Yang,[a] Jingchao Li,[a] Duo Sun,[a] Sijin Xiang,[a] Xiaolan Chen,*[a] Lanfen Chen*[b] and Nanfeng Zheng*[a]

[a]*State Key Laboratory for Physical Chemistry of Solid Surfaces, Collaborative Innovation Center of Chemistry for Energy Materials and Engineering, Research Center for Nano-Preparation Technology of Fujian Province, College of Chemistry and Chemical Engineering, Xiamen University, Xiamen 361005, China*

[b]*State Key Laboratory of Cellular Stress Biology, Innovation Center for Cell Signaling Network, School of Life Sciences, Xiamen University, Xiamen, Fujian 361102, China*

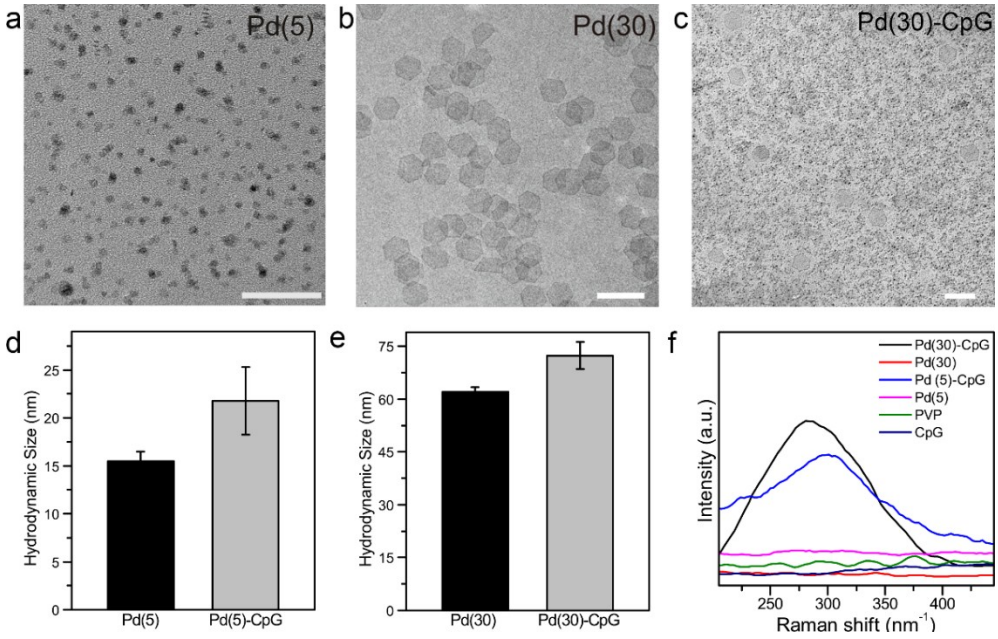

Fig. S1 TEM images of Pd(5) (a) and Pd(30) (b). (c) TEM image of negative staining of Pd(30)-CpG by using uranyl acetate. The scale bar in a, b and c was 50 nm. The hydrodynamic sizes of Pd(5) and Pd(5)-CpG (d), and Pd(30) and Pd(30)-CpG (e), respectively. (f) Raman spectra of CpG, PVP, Pd NSs and Pd-CpG in the range of 200 to 450 cm^{-1}, laser power (632 nm, 0.66 mW).

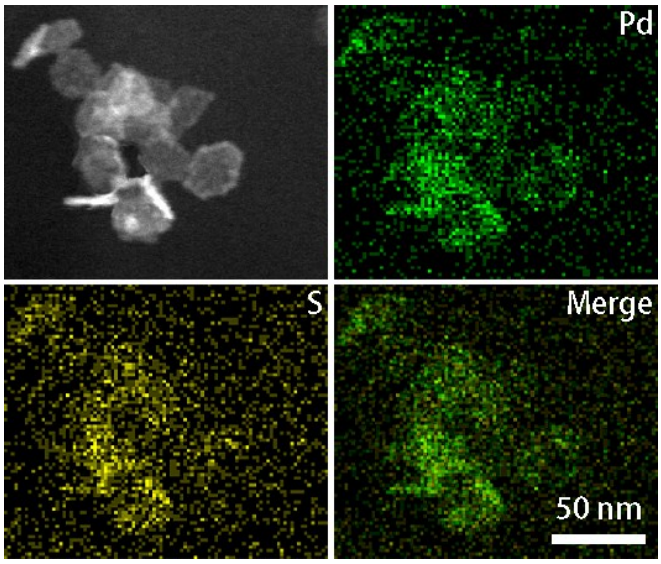

Fig. S2 HAADF-STEM-EDX mapping images of Pd-CpG.

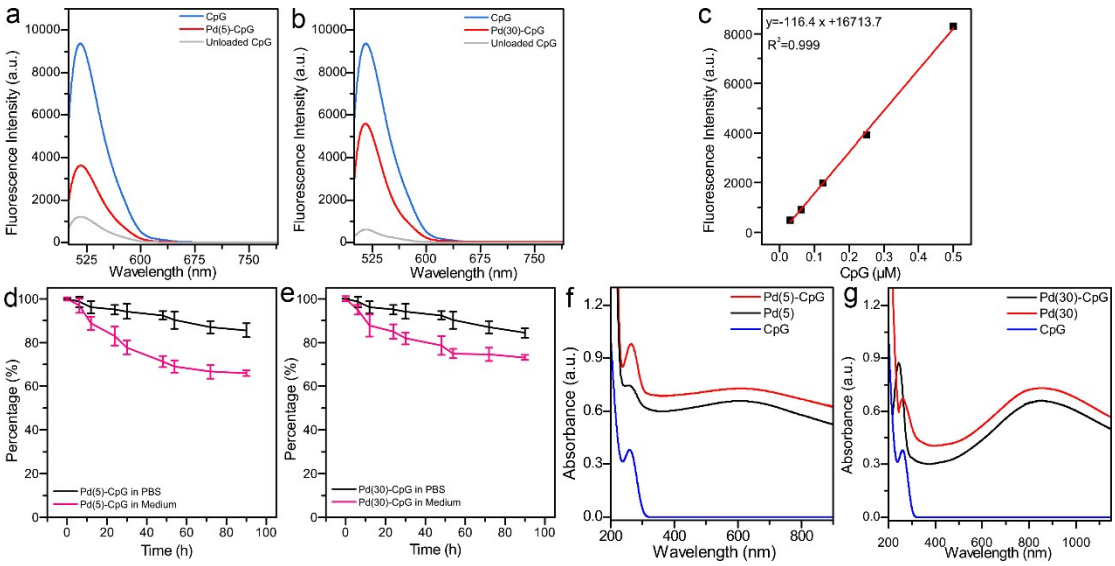

Fig. S3 (a, b) Typical fluorescence spectra of FAM-labeled CpG, Pd NSs modified with FAM-labeled CpG and the unloaded FAM-labeled CpG. (c) Standard working curve of FAM-labeled CpG relative to fluorescence intensity. The loading stability of Pd(5)-CpG (d) and Pd(30)-CpG (e) in different media (n=3 for each test). (f, g) UV–Vis–NIR absorption spectra of Pd-CpG, Pd NSs and CpG.

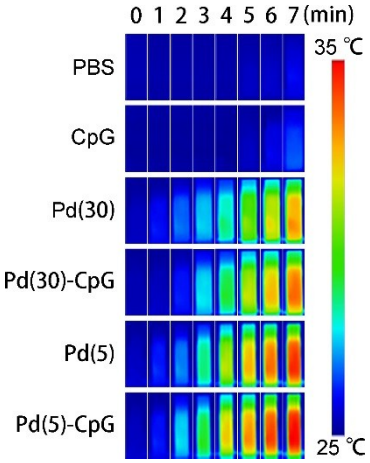

Fig. S4 The *in vitro* IR thermal images of PBS, CpG, Pd(30), Pd(30)-CpG, Pd(5) and Pd(5)-CpG upon 808 nm laser irradiation at different time intervals. The power density of 808 nm laser was 0.15 W cm^{-2} and the concentration of Pd was 25 ppm.

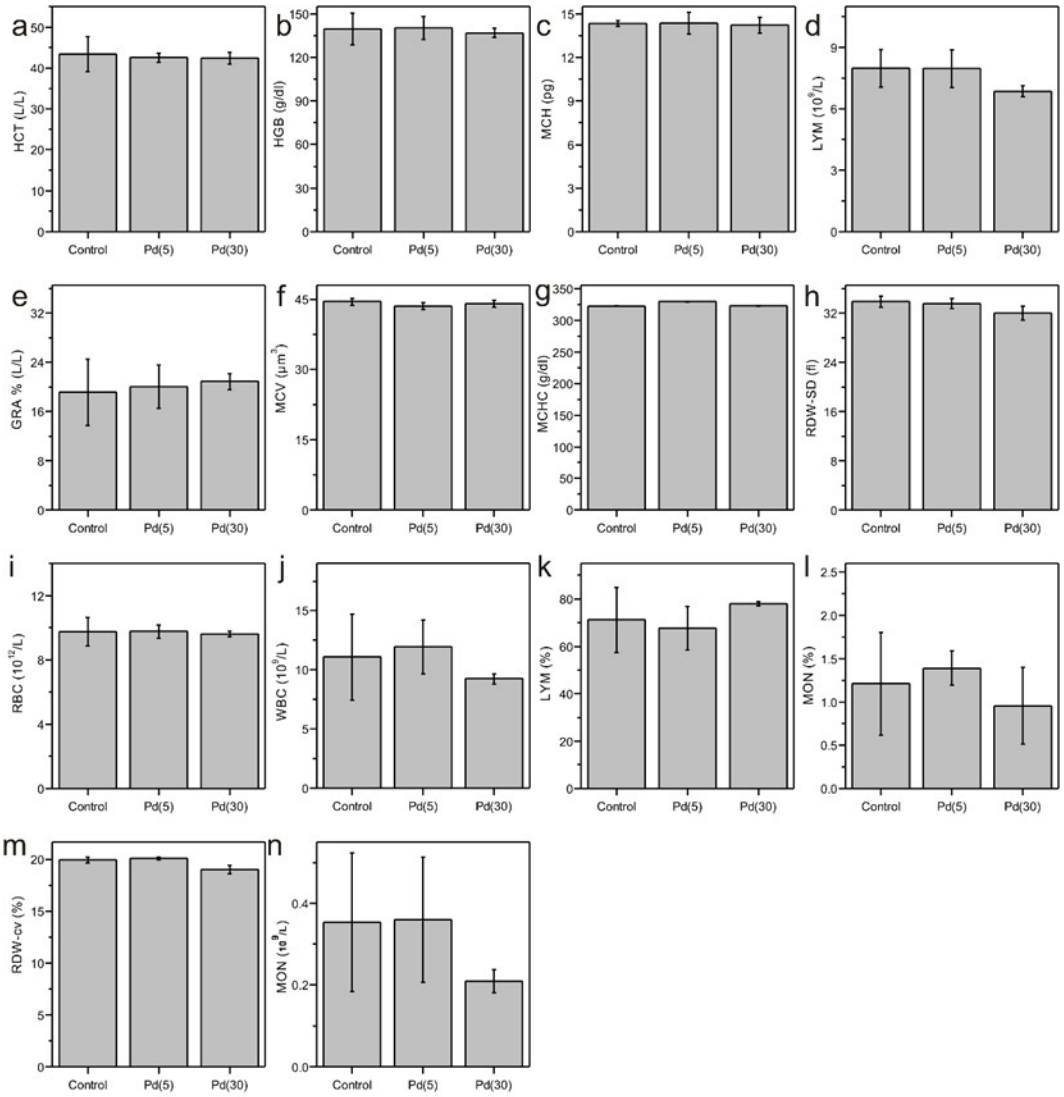

Fig. S5 Routine analysis of blood of mice treated with Pd(5) and Pd(30) after 7 days (n=3 for each group). Mean values and error bars are defined as mean and S.D., respectively.

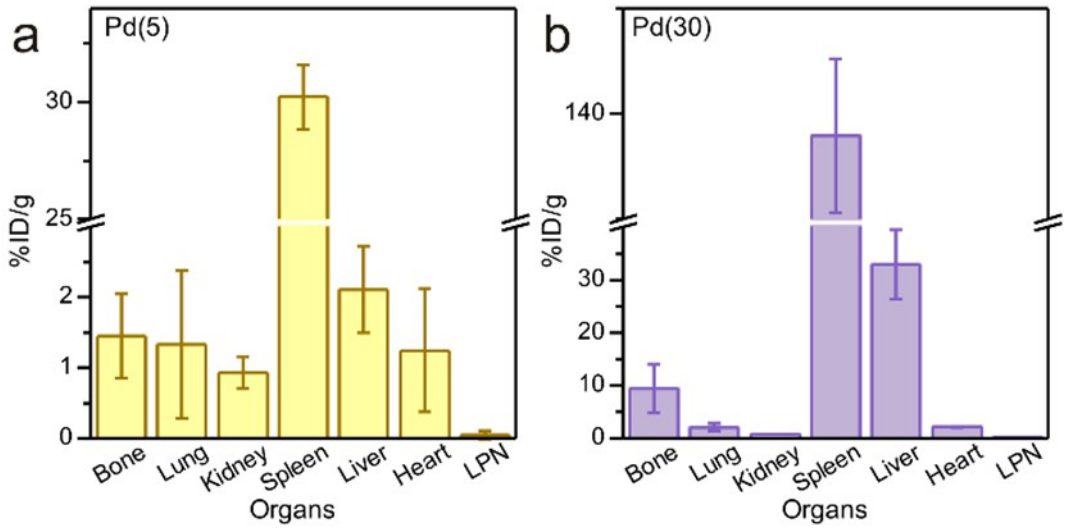

Fig. S6 The biodistributions of Pd (% injected dose (ID) of Pd per gram of tissue) in main tissues at 7 days after intravenous administration of Pd(5) (a) and Pd(30) (b) (n=3 for each group). Mean values and error bars are defined as mean and S.D., respectively.

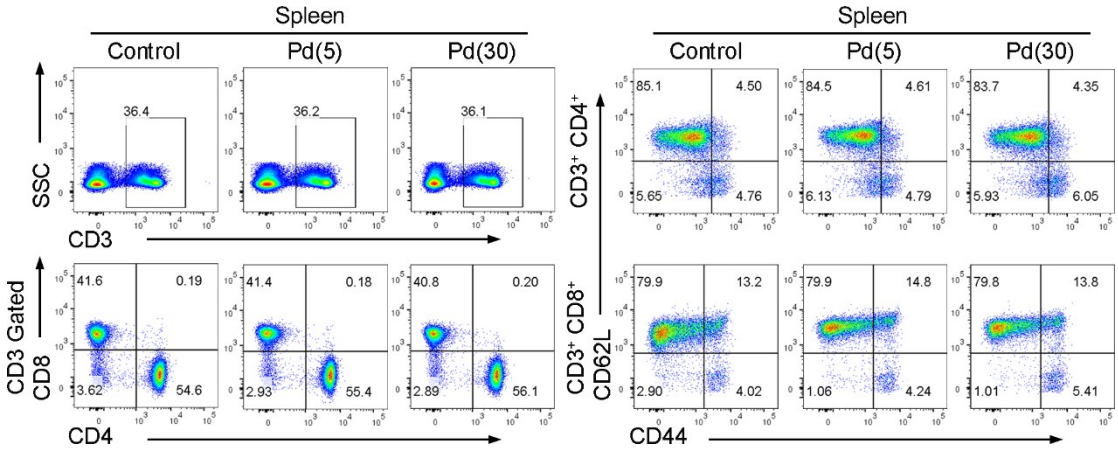

Fig. S7 Flow cytometry analysis of $CD3^+$ T cells, CD4SP ($CD3^+$ $CD4^+$ $CD8^-$)/CD8SP ($CD3^+$ $CD4^-$ $CD8^+$), $CD4^+$/$CD8^+$ Naïve T cells ($CD44^-$ $CD62L^+$), Memory T cells ($CD44^+$ $CD62L^+$), Effector T cells ($CD44^+$ $CD62L^-$) from the spleen of mice (n=3 for each group).

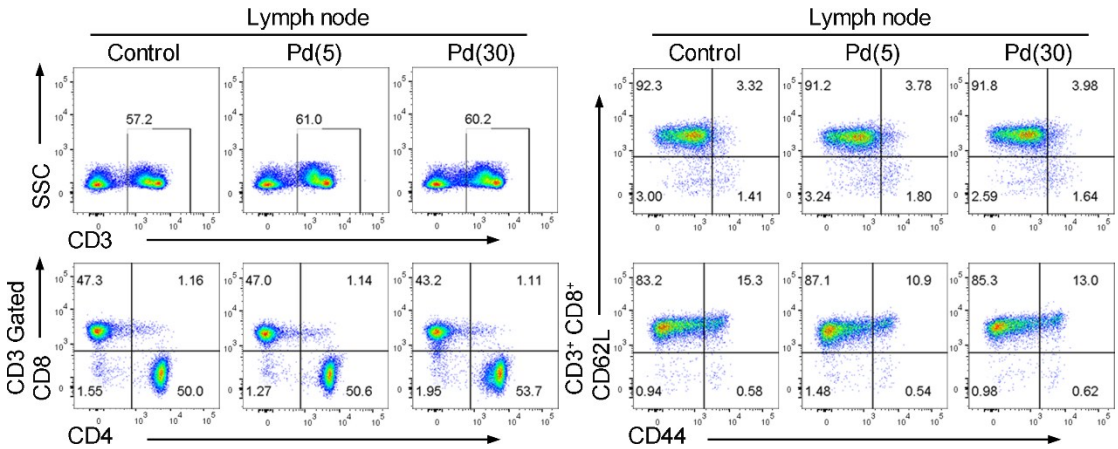

Fig. S8 Flow cytometry analysis of $CD3^+$ T cells, CD4SP ($CD3^+$ $CD4^+$ $CD8^-$)/CD8SP ($CD3^+$ $CD4^-$ $CD8^+$), $CD4^+$/$CD8^+$ Naïve T cells ($CD44^-$ $CD62L^+$), Memory T cells ($CD44^+$ $CD62L^+$), Effector T cells ($CD44^+$ $CD62L^-$) from the lymph node of mice (n=3 for each group).

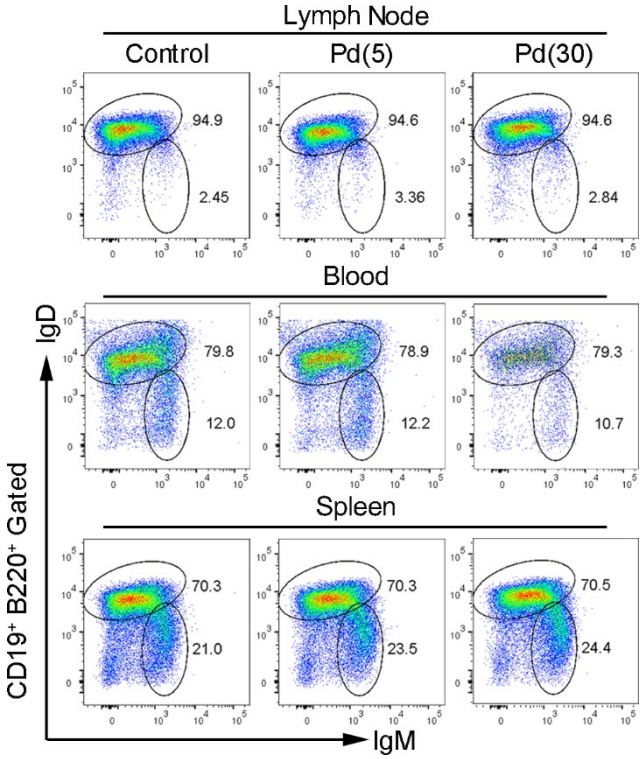

Fig. S9 Flow cytometry analysis of the maturation B cells from lymph nodes, blood and spleen of mice (n=3 for each group).

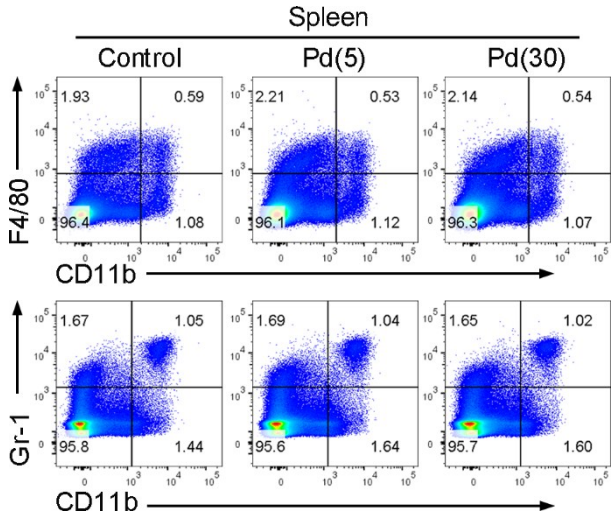

Fig. S10 Flow cytometry analysis of macrophages and neutrophils from the spleen of mice (n=3 for each group).

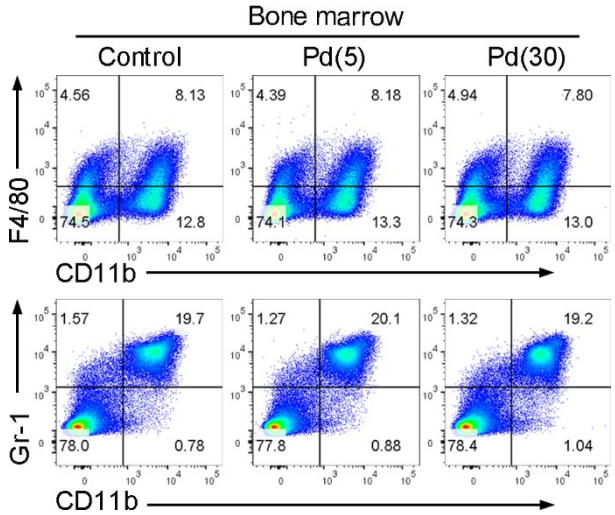

Fig. S11 Flow cytometry analysis of macrophages and neutrophils from the bone marrow of mice (n=3 for each group).

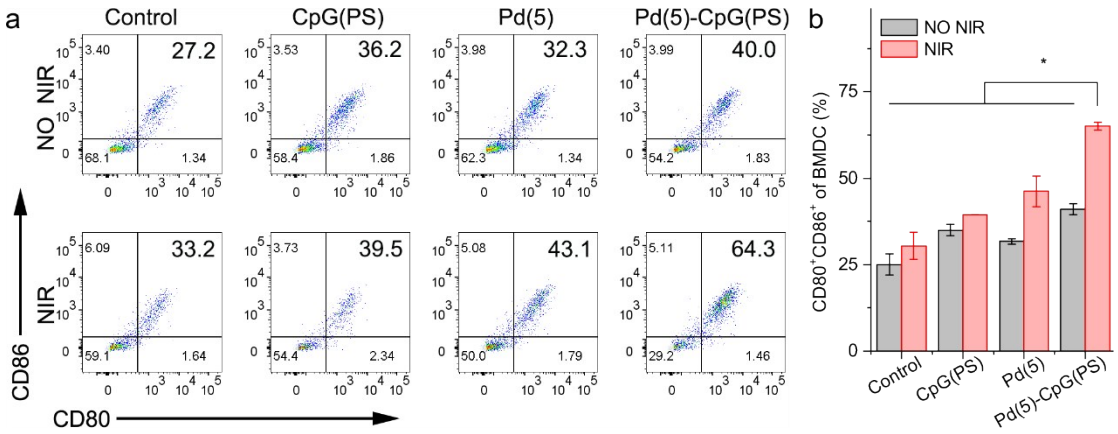

Fig. S12 Flow cytometry analysis of dendritic cell (DC) maturation after various treatments. The DC cells were stained with anti-CD80 and anti-CD86 (n=3 for each group). *p<0.05.

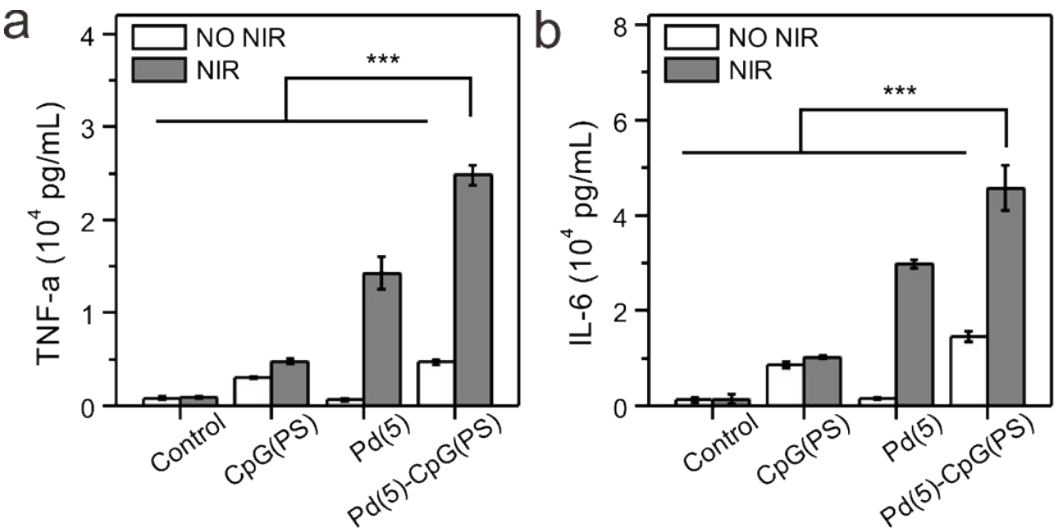

Fig. S13 Comparison of the TNF-α (a) and IL-6 (b) releases in DCs culture stimulated by PBS, CpG(PS), Pd(5) and Pd(5)–CpG(PS) without or with NIR irradiation (808 nm, 0.15 W cm^{-2}, 5 min), respectively.

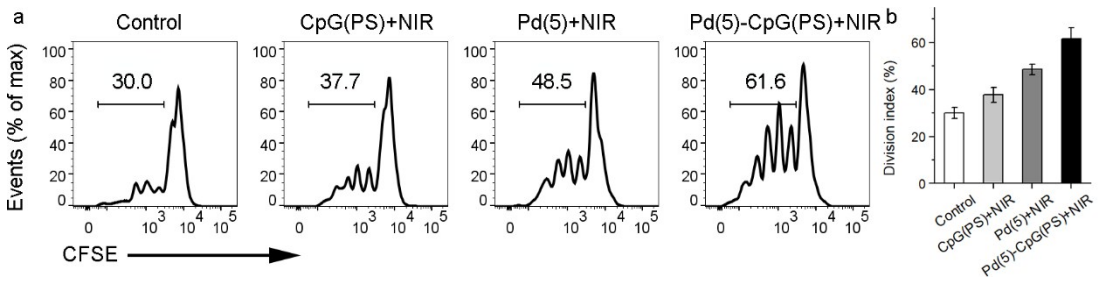

Fig.S14 The activation of $CD8^+$ T cells stimulated by matured DCs. DCs were first incubated with supernatant from Pd(5)-CpG(PS)+NIR treated B16F10-OVA (or other controls). BMDCs were then subjected to an *in vitro* presentation assay using CFSE-labeled $CD8^+$ T cells (n=4 for each group).

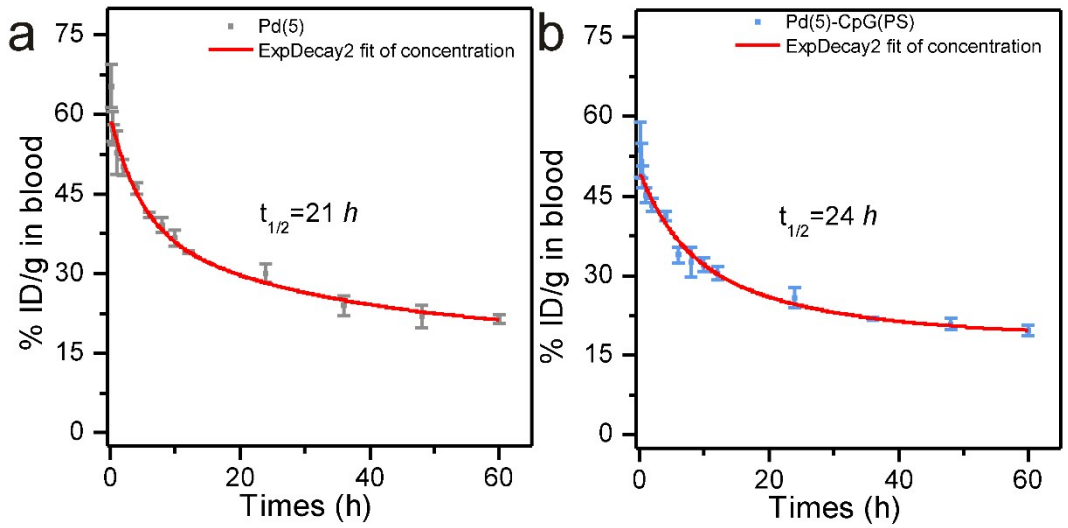

Fig. S15 Pharmacokinetics studies of Pd(5) and Pd(5)-CpG(PS). The blood circulation curves of intravenously injected Pd(5) (a) and Pd(5)-CpG(PS) (b) (n = 5). The half-lives (t1/2) for Pd(5) and Pd(5)-CpG(PS) were calculated to be ~21 h and ~24 h, respectively.

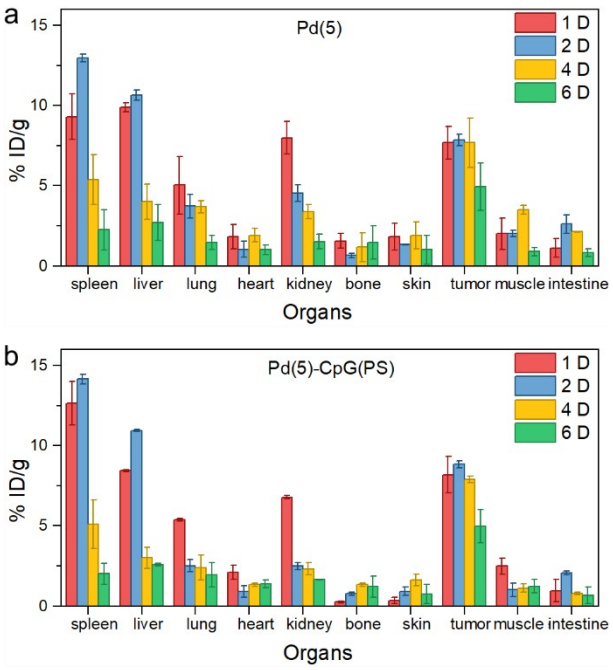

Fig. S16 The biodistributions of Pd (% injected dose (ID) of Pd per gram of tissue) in main tissues and tumors in 1, 2, 4 and 6 days after intravenous administration of Pd(5) (a) and Pd(5)-CpG(PS) (b). Mean values and error bars are defined as mean and S.D., respectively (n=5).

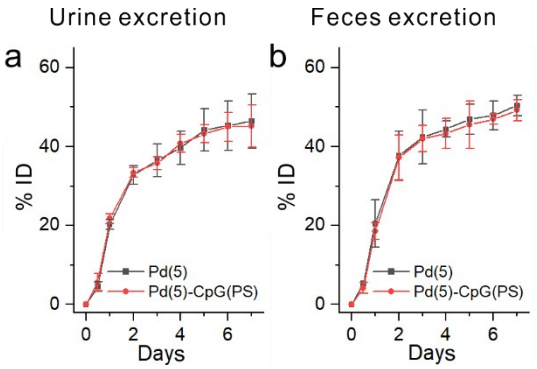

Fig. S17 Urine and feces excretion of Pd(5) and Pd(5)-CpG(PS) (n=3).

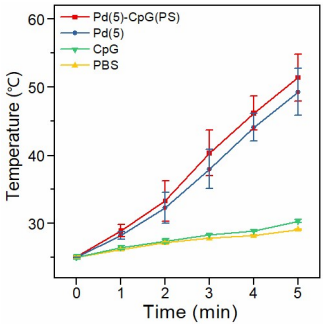

Fig. S18 The temperature increase profiles of tumor tissues in mice during laser irradiation. The power density of 808 nm laser was 0.15 W cm^{-2}.

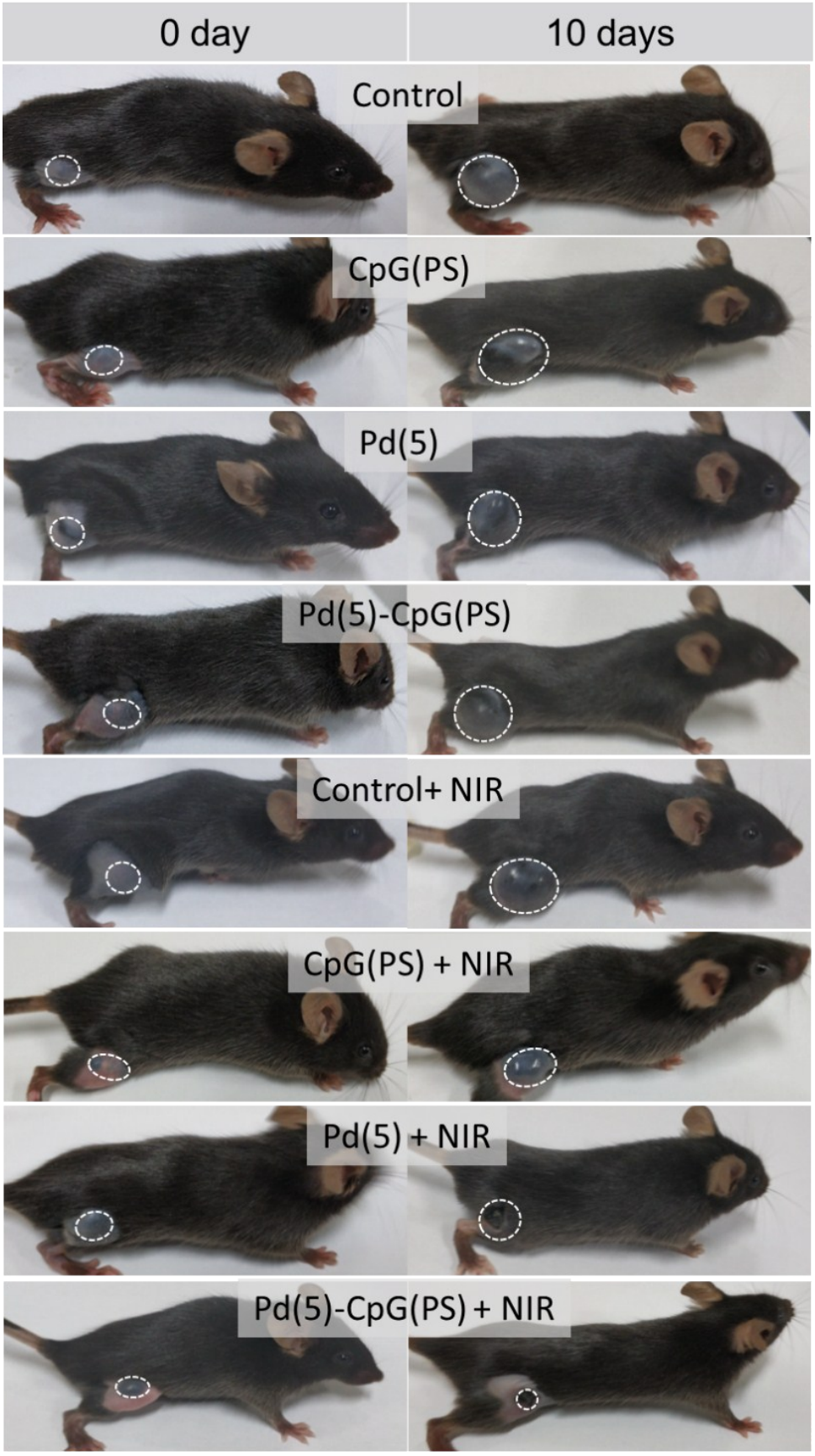

Fig. S19 Optical photos of mice before and after treatment at different treated groups.

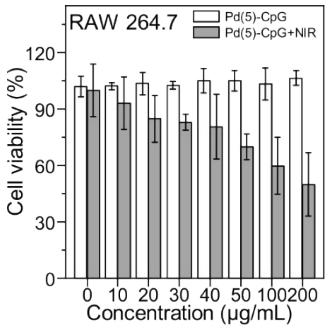

Fig. S20 PTT effect of Pd(5)-CpG on RAW 264.7 cells. The laser power density of 808 nm was 0.15 W cm^{-2}.

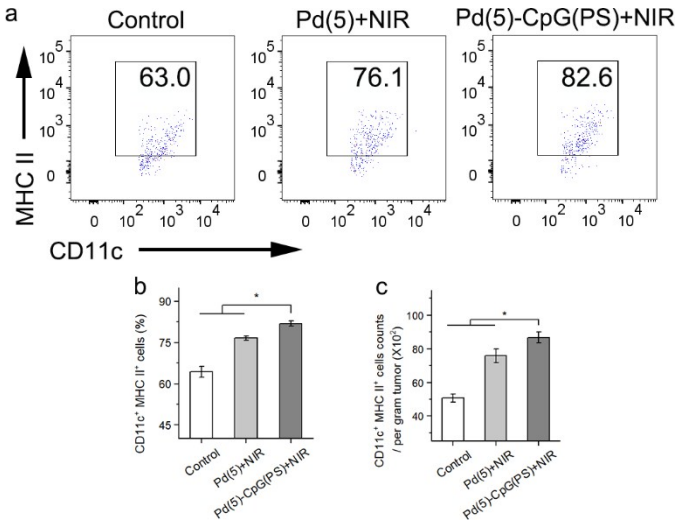

Fig. S21 The matured APCs ($CD11c^{+}MHC\ II^{+}$) both in percentage (b) and number (c) in tumor after different treatments (n=4 for each group).

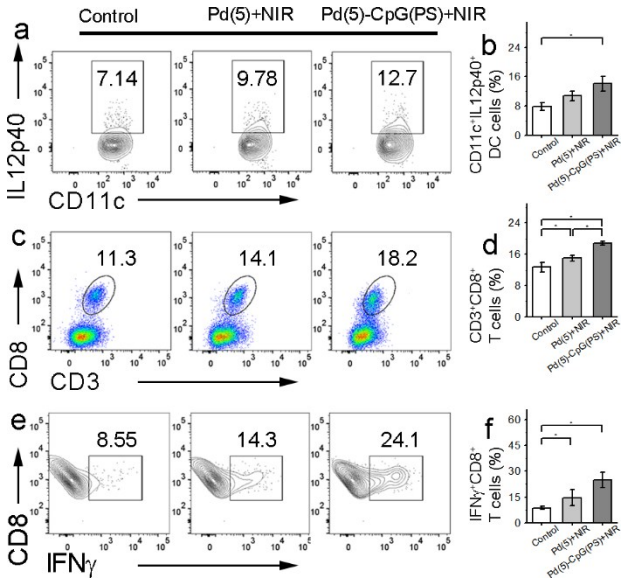

Fig. S22 $CD11c^+$ $IL12p40^+$ cells (a and b), $CD3^+$ $CD8^+$ cells (c and d) and IFNγ $CD8^+$ cells (e and f) from the spleen of mice (n=4 for each group).

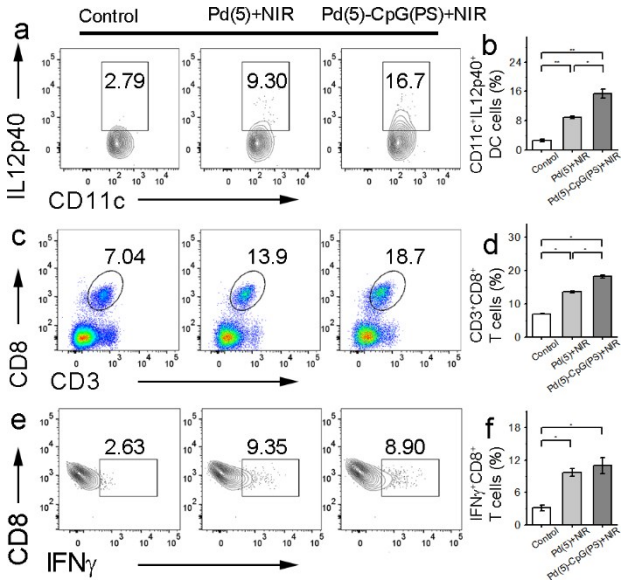

Fig. S23 $CD11c^+$ $IL12p40^+$ cells (a and b), $CD3^+$ $CD8^+$ cells (c and d) and IFNγ $CD8^+$ cells (e and f) from the blood of mice (n=4 for each group).

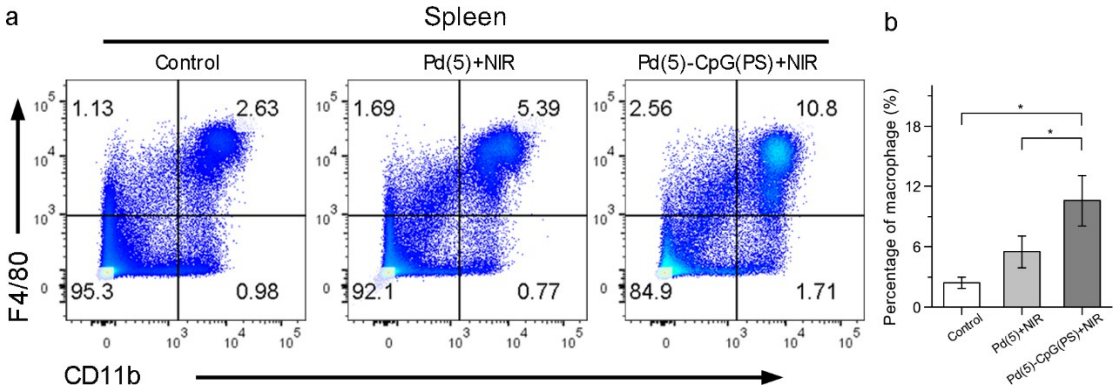

Fig. S24 Flow cytometry analysis of macrophage (a and b) from the spleen of mice (n=4 for each group).

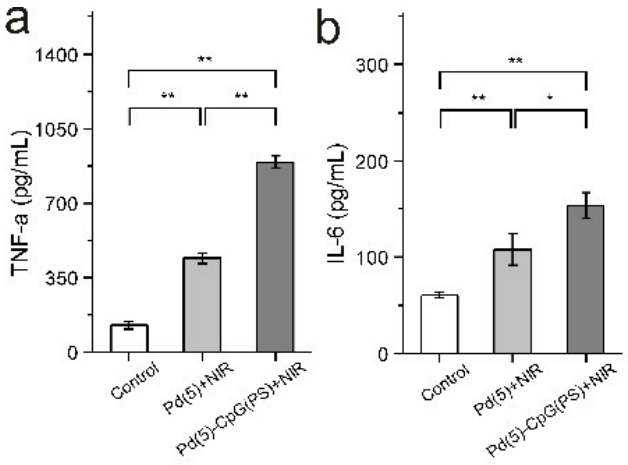

Fig. S25 Concentrations of TNF-α (a) and IL-6 (b) in the sera of different groups treated mice (Control, Pd(5)+NIR and Pd(5)-CpG(PS)+NIR).

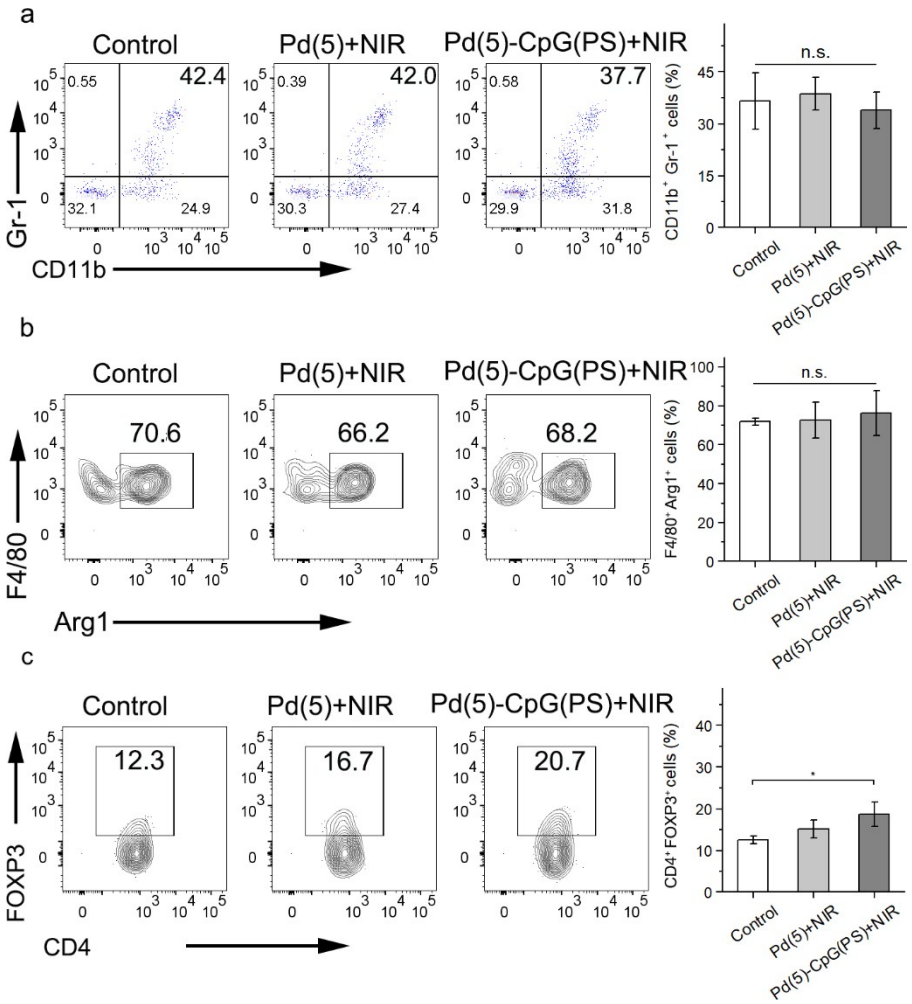

Fig. S26 Flow cytometry analysis of MDSCs ($CD11b^+Gr\text{-}1^+$), M2 macrophages ($Arg1^+F4/80^+$) and Treg cells ($CD4^+FOXP3^+$) in tumor after Pd(5)+NIR and Pd(5)-CpG(PS)+NIR treatment (n=4 for each group).